

Demonstration of the International Space Station Particle Database Website

Nathalie Tuya¹, Wenyan Li², and Luz M. Calle³
NASA, Kennedy Space Center, FL, 32899

Marit E. Meyer⁴
NASA Glenn Research Center, Cleveland, Ohio, 44135

Meytar Sorek-Hamer⁵

Universities Space Research Association, Mountain View, California, 94035
NASA Ames Research Center, Moffett Field, Mountain View, California, 94035
and

Irina Hallinan⁶

Universities Space Research Association, Mountain View, California, 94035
NASA Ames Research Center, Moffett Field, Mountain View, California, 94035

NASA has continuously emphasized the importance of allowing the public to interact and engage with its missions and initiatives by using open-source data. As a result of the large dataset gathered during the International Space Station (ISS) aerosol sampling missions, the ISS Aerosol Sampling Experiment Web Application was developed. This application allows users to easily plot and visualize data from the 2016 and 2018 aerosol experiments. This tool is a public-facing website, allowing anyone to easily plot the ISS aerosol data in order to develop their own research and conclusions. This platform allows for plotting and visualization of particle composition, geometry, morphology, sampling durations, and collection locations. The tool features an elemental composition pie chart, a plot tool, and an interactive plot tool. The work presented on this paper involves a demonstration of how this Web Application was used to show the morphology of aluminum-chlorine-zirconium particles as well as the presence of lead particles on Node 3 and Node 2 of the ISS.

Nomenclature

<i>ISS</i>	=	International Space Station
<i>SEM</i>	=	Scanning electron microscopy
<i>CCSEM</i>	=	Computer controlled scanning electron microscopy
<i>EDS</i>	=	Energy dispersive spectroscopy
<i>NASA</i>	=	National Aeronautics and Space Administration

¹ NASA Intern and Columbia University PhD Candidate, New York, NY 10027.

² LASSO Contract Research Scientist, Kennedy Space Center, FL 32899.

³ NASA Senior Research Scientist, Exploration Systems & Development Office, Mail Code: UB-E, Kennedy Space Center, FL, 32899.

⁴ NASA, Research Aerospace Engineer, Low-Gravity Exploration Technology Branch, 21000 Brookpark Road, Cleveland, OH 44135

⁵ NASA Research Scientist, Ames Research Center, Environmental Analytics Group, Mountain View, CA 94035.

⁶ Software Engineer, Universities Space Research Association at Ames Research Center, NASA Academic Mission Services, Mountain View, CA 94035.

TEM = Transmission electron microscope
Z = Atomic number
OSHA = Occupational Safety and Health Administration

I. Introduction

THE International Space Station (ISS) has been receiving crews since the year 2000. On the ISS, airborne particulate matter, or, aerosols, of various diameters are able to freely float throughout the station since they do not undergo gravitational settling. The presence of such aerosols are commonly discussed by ISS crewmembers^{1,2}, yet they remain understudied. As a result, the Aerosol Sampling Experiments, conducted in 2016 and 2018, sought to investigate the aerosols present on the ISS^{3,4,5}. These experiments utilized both Passive Samplers (PAS) and Active Samplers (AAS) to obtain a wide size range of aerosols. The PAS collection substrate consists of a black carbon sticky tape onto which particles adhere to. The AAS uses a TEM grid substrate. In 2016, seven PASs were placed on various ISS air vent filters throughout the station, and allowed to collect particles for 2, 4, 8, 16, 26, and 32 days. After collection, the samplers were sent back to Earth and the optimal substrate from each PAS underwent analysis using scanning electron microscopy (SEM), computer-controlled SEM (CCSEM), and energy dispersive spectroscopy (EDS). The samples were distinctly different from typical aerosols sampled from indoor spaces on Earth. The most remarkable aspect were the many different metals and multi-component particles with individual metal inclusions within a carbonaceous matrix. Consequently, a metals analysis was the first approach to CCSEM on one substrate from each PAS, followed by an analysis of all particles (carbon and metals) for one ISS location. The results of these analyses resulted in an abundance of data on both individual particles and on metal inclusions in particles, including elemental composition and morphology. The repeat sampling experiment in 2018 augmented the data set and improved the statistics by exposing sampling substrates for five PASs on vents for 26 days and analyzing all the samples.

NASA has continuously emphasized the importance of allowing the public to interact and engage with its missions and initiatives through the use of open-source data⁶. As a result of the large dataset developed through the ISS aerosol missions, the International Space Station Aerosol Sampling Experiment web application⁷ was created. This application, openly accessible on <https://iss-particle-db.arc.nasa.gov>, allows users to easily plot and visualize data from the 2016 and 2018 aerosol experiments. This tool allows researchers, teachers, students and the scientifically curious to easily plot the ISS aerosol data to learn about indoor air quality in spacecraft.

II. Data Overview

A. Sampler Data

In 2016, eleven samples were selected for CCSEM analysis, as described in *Table 1*. These samples were selected based on having sufficient particle coverage on the sampling substrate. If particles are too crowded, then the edges overlap and it is difficult to determine where one particle ends and another begins. If particles are too sparsely loaded, then it is difficult to do CCSEM, and manual microscopy is preferred. The first analysis on the ISS samples was conducted on metal particles and metal inclusions within particles. CCSEM requires a user-defined lower size limit for the analysis, which was determined to be 1 μm for optimal performance. Smaller particles would require analysis by manual microscopy and the additional cost was not prioritized because the AAS TEM grids targeted that size range. In SEM backscattered electron images, high atomic number materials tend to have higher contrast against the black carbon tape substrate vs. the grey-scale carbon and lower atomic number particles, therefore, only metals with an atomic number, Z , greater than or equal to 22 (titanium) were targeted to improve edge detection.

For the 2018 experiment, all the substrates were exposed for 26 days and they all had sufficient particle coverage. These were analyzed in the same manner as the 2016 sample set.

Another analysis type included all particles with measured diameters of 5 μm and larger (carbonaceous and metals). The lower size threshold made the analysis feasible, when considering the edge detection challenges of grey-scale carbon particles. In the 2016 analysis, the PAS at NOD3D3 was selected for this analysis since all five of the different sampling day substrates had suitable coverage for CCSEM. The 2-day sample had sufficient particles for a good analysis, and the 32-day sample was not too heavily loaded. For the 2018 payload, one substrate from the PAS at LAB1PD3 was selected for the same analysis. Through CCSEM, values for particle size, morphological characteristics, and elemental composition were obtained.

Table 1. Passive Sampler substrates analyzed using CCSEM.

LOCATION	NOTATION	ACTIVITIES	SAMPLING Duration
Node 1 Deck 3	NOD1D3	Eating Area	16, 26*
Node 3 Deck 3	NOD3D3	Hygiene + Exercise	2, 4, 8, 16, 26, 32
Permanent Multipurpose Module (PMM) [†]	PMM	Storage	32
Node 2 Deck 3	NOD2D3	Crew Sleep + Vehicle Docking	26, 32
Node 3 Forward 3	NOD3F3	Hygiene + Exercise	8, 26
US Lab Bay 1 Port/Deck Standoff [†]	LAB1SD1	Experiments	32
US Lab Bay 3 Port/Deck Standoff	LAB1PD3	Experiments	16, 26

*All 2018 samples were left out for 26 days

[†]Location was only sampled in 2016

The ISS Aerosol Sampling web application contains information on 5738 metal particles from 2016 and 48,740 particles from 2018, for a combined total of 54,477 particles grouped into 78 particle classes. Each particle has unique values for elemental composition, morphology, and size. *Figure 1* provides a demonstration of the abundance of data from both the 2016 and 2018 experiments. It must be emphasized that these particles may not be free-floating and may be metal inclusions in larger complex particles. There are significantly more particles from the 2018 experiment because all substrates were exposed for 26 days, a duration chosen based on the results of the first sampling. On Earth, aerosol sampling is typically an iterative process and may take many attempts before the optimal sampling duration is achieved. Fortunately, the range of different exposure times (based on an initial guess) for 2016 sampling yielded a definitive range for good particle coverage across all the different locations.

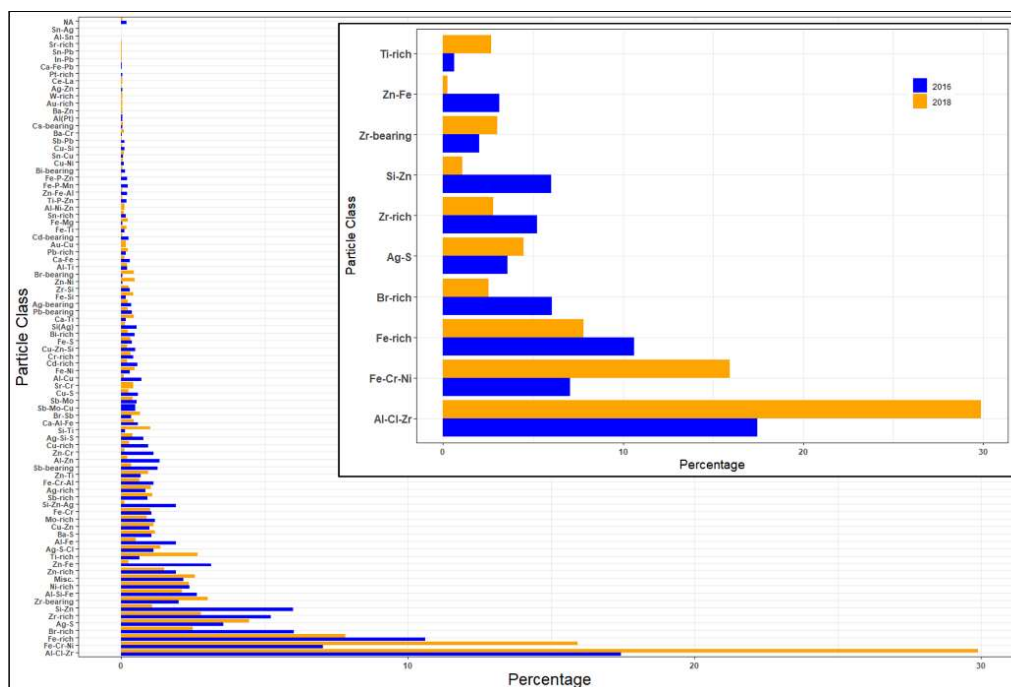


Figure 1. Comparison of the 2016 and 2018 results of all particles in the ISS Aerosol Sampling web application database. The weight percentage of each particle class (out of 100% for sample set) is plotted, with the ten most abundant particle classes shown in the inset

B. Computer Controlled Scanning Electron Microscopy

Computer controlled scanning electron microscopy, or CCSEM, was used to analyze the aerosol samples. Specifically, IntelliSEM⁸, a program developed by the RJLee Group, was utilized. With CCSEM, the process of finding and characterizing particles from an SEM image becomes automated, providing a more comprehensive dataset⁹. The core processes of CCSEM include particle detection, size and shape measurement, and determination of elemental composition is simultaneously acquired from EDS.

Particle detection and measurement is accomplished by using the backscattered electron (BE) mechanism of image formation. With this technique, heavier elements appear brighter. Image analysis techniques using pixel color contrast can detect the edges of the particles and measure multiple geometric parameters. Once particles are measured and detected, EDS is used to determine the elemental composition of each particle. Energy of each x-ray photon is measured and the sum of counts is compiled into a spectrum, such as in Figure 2. The location of peaks correspond to the elements present and the size of the peaks can, in some cases, inform the relative abundance of these elements in the particle analyzed. The silver particle shown in Figure 2 is a high-resolution micrograph imaged by manual microscopy (separate from the CCSEM analyses). Some representative particles from different particle classes were chosen for more detailed study but are not included in the website.

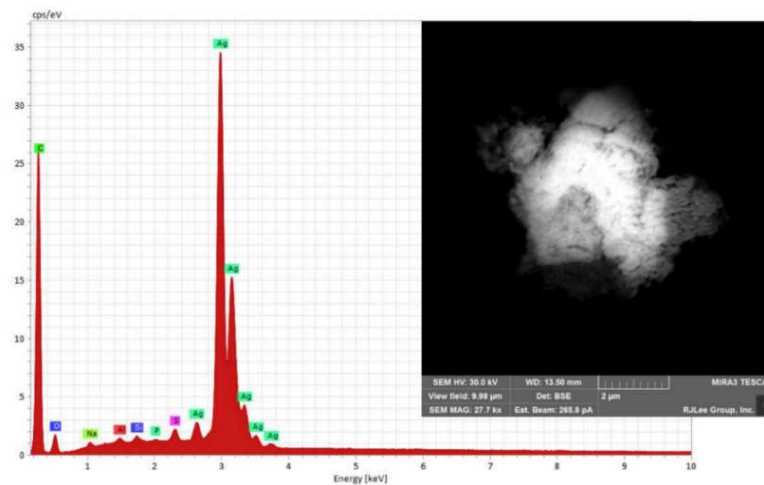


Figure 2. High Resolution SEM micrograph from manual microscopy of a silver particle along with its respective EDS spectrum

Summarizing the CCSEM results is simplified by the creation of particle classes. These are formed by applying user-defined rules that are based on the relative abundance of elements and frequently occurring combinations of these elements in the sampled particles. In order to keep a data set manageable, there should be no more than 60 to 70 distinct particle classes. The classes chosen for one analysis may not be suitable for subsequent analyses and will depend on the randomness and statistics of each individual sampling results. Some particles do not get their own particle class, for example, if there are only one or two particles that are similar and cannot logically be grouped into other classes, these will be in the category ‘miscellaneous.’ Some particle classes have nearly the same names, such as Ag-rich and Ag-bearing, which are based on the relative abundance of Ag outlined in the user-defined particle class rules. A more detailed explanation of particle class rules can be found in Ley et al. that examined silver particles on ISS. The website currently has 78 particle classes because the two individual analyses from 2016 and 2018 were combined for comparison purposes. This is subject to change in the event that future sampling results are added to the site.

III. Website Features

The website includes many options of visualizing the data without downloading it. The user has an option to create plots and can control the plotting attributes. Several interactive features exist within the ISS aerosol website across tabs. These include the elemental composition pie chart, the plot, and the interactive plot. The elemental composition pie chart provides an overview of the most abundant particle classes found at specific ISS locations and sampling times. The plot and interactive plot tool visualize data in the form of a scatter plot, boxplot, density plot, mean and error bar plot, and a histogram. Particles can be plotted based on different particle morphology parameters as well as by particle abundance in the sample. This allows users flexibility when assessing for trends in the data.

The public website (<https://iss-particle-db.arc.nasa.gov/>) was developed using the combination of R programming language, JavaScript, HTML, and CSS. The website has a responsive and modern interface. Widely used open-source packages were used and extended to build the interactive website, including Shiny, ggplot2, and plotly. The “App Info” tab of the site contains a more detailed description of the packages used to make the site. The website was deployed using RStudio Connect software and runs on the web servers, hosted by the NASA Ames Code-I Managed Cloud Environment.

A. Elemental Composition Pie Chart

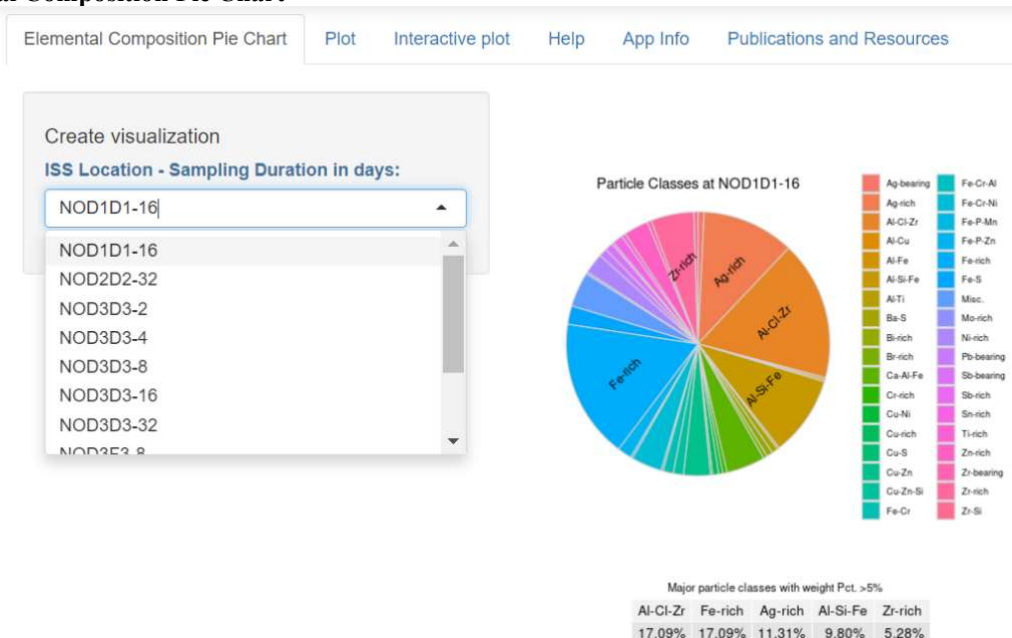


Figure 3. Elemental composition pie chart for NOD3D3-32. ISS Locations and sampling durations are selected from the dropdown menu on the left.

The Elemental Composition Pie Chart uses a color-coded pie chart to plot the overall weight percentage of each elemental particle class for each sampler and its respective sampling duration. The dropdown menu allows the choice of the location, followed by the number of days the sampling substrate was exposed. It also displays a table at the bottom showing a weight percentage value for those particle classes that have a weight greater than or equal to 5%.

B. Plot Options

The plot tool features several different types of graphs to visualize the aerosols. These include a scatter plot, box-and-whisker plot, mean and error bar plot, and a histogram. Examples of some of these visualizations are shown in *Figure 4*. Note that future changes to the website may result in differences in format and plotting options.

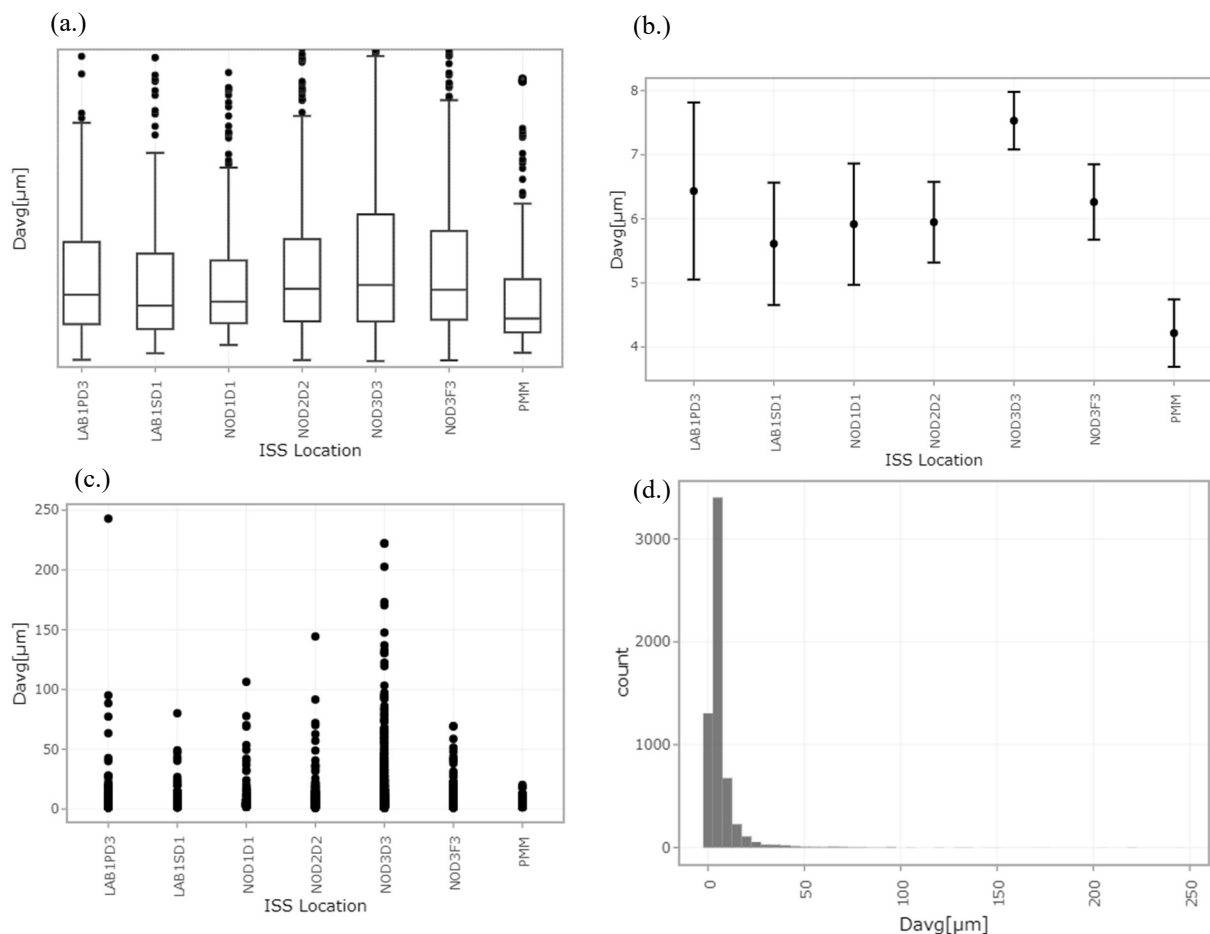


Figure 4. Examples of plot visualizations. (a) Box-and-whisker plot of average diameter by sampler location (b) Mean + error bar of average diameter by sampler location (c) Scatter plot of average diameter by plot location (d) Histogram of average diameter

The boxplot, also called a box-and-whisker plot, displays the mean as the center line, the 25th and 75th percentile as the top and bottom lines of the box, and minimum and maximum with the vertical error bars. Outliers are displayed as points, as seen in *Figure 4a* on the NOD1D3 and NOD3D3 plots. The boxplot also has the option to show all the individual particle data points overlaid atop the boxplot. The mean + error plot displays the mean as the center point and the associated standard error as the vertical lines. The scatter plot displays all of the available data to show the relationship between the two variables selected. The histogram displays the frequency of the given variable per 'bin' value. The bin value, also known as the interval, divides the data in groups based on if they fit the range of the specified interval. The interval can be adjusted by the user to achieve the desired visualization.

Several particle-related variables are available to plot on the web application. Particle morphology parameters are quantified in CCSEM and selected variables can be plotted using the tool. These include average diameter, aspect ratio, volume, and roundness. In addition to particle morphology statistics, the percentage of each element in the particle can be plotted by selecting any of the available elements shown in *Figure 5* from the plot dropdown menus. The aforementioned variables can be plotted on the y- or x-axes, and a ‘group’ variable can be added to include a third dimension to the plot when applicable (note that some group variables can be plotted but are not necessarily meaningful for every combination of x- and y-variables). Other variables that can be plotted on the y-axis or as a group include particle class, ISS location, ISS location duration (the location code followed by a hyphen and the number of sampling days), and each individual element (the magnitude reflects the relative net x-ray counts).

1 IA H Hydrogen 1.008	2 IIA He Helium 4.0026																
3 Li Lithium 6.941	4 Be Beryllium 9.0122											5 B Boron 10.811	6 C Carbon 12.011	7 N Nitrogen 14.007	8 O Oxygen 15.999	9 F Fluorine 18.998	10 Ne Neon 20.180
11 Na Sodium 22.990	12 Mg Magnesium 24.305											13 Al Aluminum 26.982	14 Si Silicon 28.086	15 P Phosphorus 30.974	16 S Sulfur 32.06	17 Cl Chlorine 35.45	18 Ar Argon 39.948
19 K Potassium 39.098	20 Ca Calcium 40.078	21 Sc Scandium 44.956	22 Ti Titanium 47.88	23 V Vanadium 50.942	24 Cr Chromium 51.996	25 Mn Manganese 54.938	26 Fe Iron 55.845	27 Co Cobalt 58.933	28 Ni Nickel 58.693	29 Cu Copper 63.546	30 Zn Zinc 65.38	31 Ga Gallium 69.723	32 Ge Germanium 72.63	33 As Arsenic 74.922	34 Se Selenium 78.96	35 Br Bromine 79.904	36 Kr Krypton 83.798
37 Rb Rubidium 85.468	38 Sr Strontium 87.62	39 Y Yttrium 88.906	40 Zr Zirconium 91.224	41 Nb Niobium 92.906	42 Mo Molybdenum 95.94	43 Tc Technetium 98	44 Ru Ruthenium 101.07	45 Rh Rhodium 102.905	46 Pd Palladium 106.42	47 Ag Silver 107.868	48 Cd Cadmium 112.411	49 In Indium 114.818	50 Sn Tin 118.710	51 Sb Antimony 121.757	52 Te Tellurium 127.6	53 I Iodine 126.905	54 Xe Xenon 131.29
55 Cs Cesium 132.905	56 Ba Barium 137.327	57-71 Lanthanoids	72 Hf Hafnium 178.49	73 Ta Tantalum 180.948	74 W Tungsten 183.84	75 Re Rhenium 186.207	76 Os Osmium 190.23	77 Ir Iridium 192.222	78 Pt Platinum 195.084	79 Au Gold 196.967	80 Hg Mercury 200.59	81 Tl Thallium 204.38	82 Pb Lead 207.2	83 Bi Bismuth 208.98	84 Po Polonium 209	85 At Astatine 210	86 Rn Radon 222
87 Fr Francium 223	88 Ra Radium 226	89-103 Actinoids	104 Rf Rutherfordium 261	105 Db Dubnium 262	106 Sg Seaborgium 266	107 Bh Bohrium 264	108 Hs Hassium 277	109 Mt Meitnerium 268	110 Ds Darmstadtium 271	111 Rg Roentgenium 272	112 Cn Copernicium 285	113 Nh Nihonium 284	114 Fl Flerovium 289	115 Mc Moscovium 288	116 Lv Livermorium 293	117 Ts Tennessine 294	118 Og Oganesson 294
57 La Lanthanum 138.905	58 Ce Cerium 140.12	59 Pr Praseodymium 140.908	60 Nd Neodymium 144.24	61 Pm Promethium 145	62 Sm Samarium 150.36	63 Eu Europium 151.964	64 Gd Gadolinium 157.25	65 Tb Terbium 158.925	66 Dy Dysprosium 162.50	67 Ho Holmium 164.930	68 Er Erbium 167.259	69 Tm Thulium 168.934	70 Yb Ytterbium 173.054	71 Lu Lutetium 174.967			
89 Ac Actinium 227	90 Th Thorium 232.038	91 Pa Protactinium 231.036	92 U Uranium 238.029	93 Np Neptunium 237	94 Pu Plutonium 244	95 Am Americium 243	96 Cm Curium 247	97 Bk Berkelium 247	98 Cf Californium 251	99 Es Einsteinium 252	100 Fm Fermium 257	101 Md Mendelevium 258	102 No Nobelium 259	103 Lr Lawrencium 260			

Figure 5. Elements available to plot on database. Note that elements less than or equal to atomic number 22 exist in combination with of other elements, but the CCSEM edge detection threshold targeted brighter particles (titanium and higher atomic number) so individual particles solely comprised of these elements were not included in the analysis.

The ‘facet row’ and ‘facet column’ features allow for additional organization of data. These allow for one to “split” up the data by either particle class, ISS location, ISS location with time, or heavy metals. The facet row organizes the data horizontally, while the facet column splits it vertically. *Figure 6* shows an example with all of the variable features of the plot tool utilized, as well as a screenshot of the ‘Plot’ user interface.

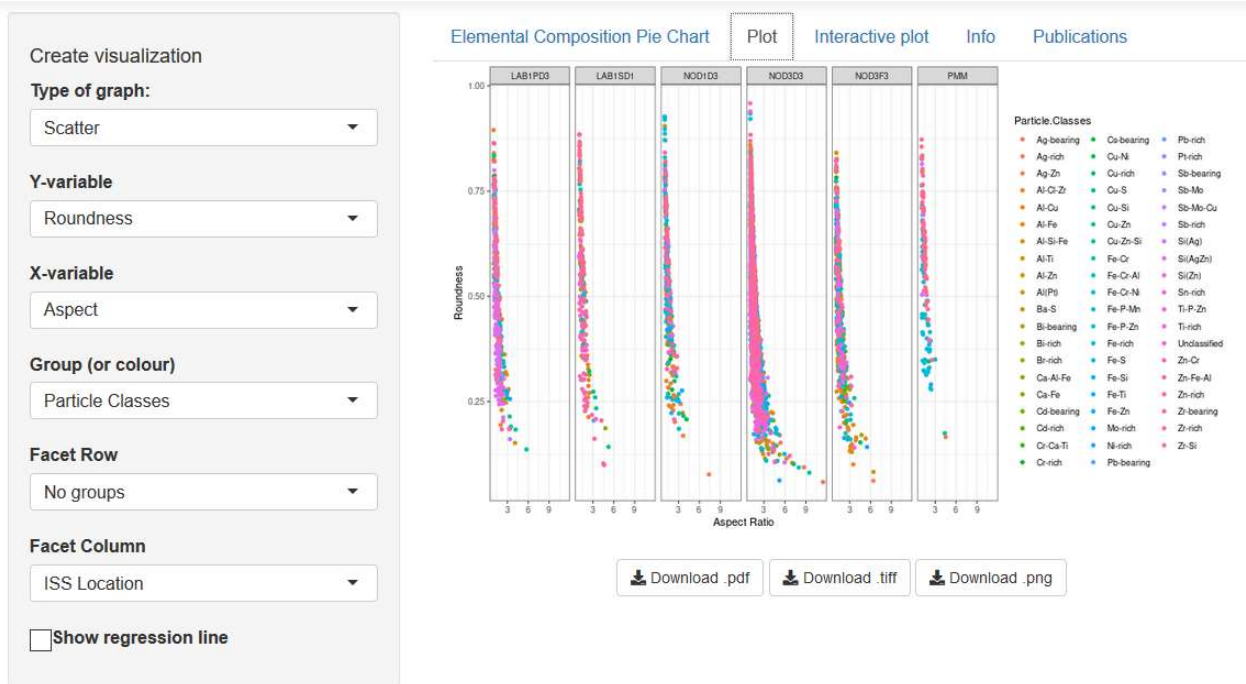


Figure 6. Plot with Group and Facet Column features. Aspect ratio is plotted on the y-axis as a function of roundness on the x-axis. The data is then grouped by particle class and color-coded accordingly. Additionally, ISS location is used as a facet column to split the data

C. Interactive Plot

The interactive plot features the same functionalities of the plot tool, except that it has additional interactive elements. The most significant feature is the ability to filter by subgroup. When data is grouped, the normal plot will display all groups within the variable selected. However, with the interactive plot, one can filter out certain subgroups to create a better visualization. Single-clicking a subgroup that is already on the plot will remove it, while single-clicking a subgroup not on the plot will add it. Double clicking a group will isolate that subgroup on the plot. Double-clicking again adds all of the subgroups back onto the plot. This feature is shown in *Figure 7*.

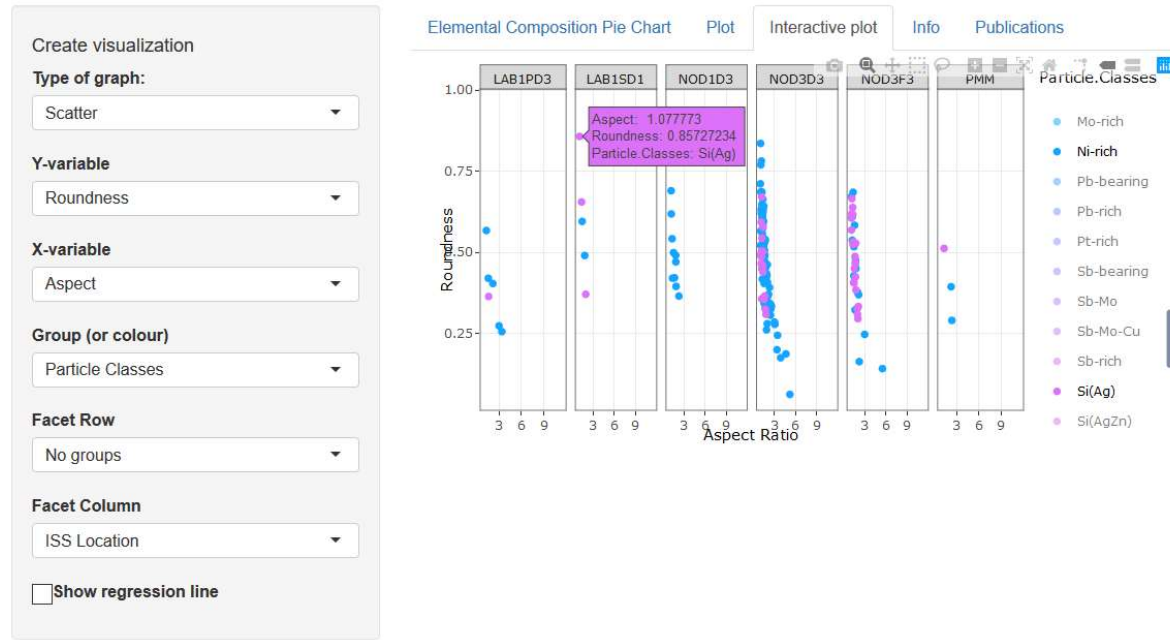


Figure 7. Interactive plot displaying only subgroups ‘Ni-rich’ and ‘Si(Ag)’. This plot is identical to the plot in *Figure 6* with the exception that only certain subgroups are displayed. The ‘hover’ feature is also displayed, which shows more detailed particle information. These are features unique to the interactive plot.

Additional interactive features include the ability to hover over a point to show more details information on that particle. A text box opens that displays exact values for the variables plotted on the x and y-axis and the group variables, as shown in *Figure 7*. Other features of the interactive plot include zooming and panning to create a better visualization. One can also select data using either the box or lasso tool. All of these features exist to better display data of interest.

D. Plot Attributes

The ‘Change Plot Attributes’ feature on the right-hand side of the graphs allows for customization of the visualizations created on the web application. The ‘Text’ tab allows for customization of axes labels, title, font size, and font. The overall appearance of the plot can be changed using the ‘Theme’ tab. The ‘Legend’ tab allows one to rename the legend, as well as remove it or change its position. The size of the plot can be adjusted on the ‘Size’ tab, either on the screen itself or for download. The entire user interface of customization options is shown in *Figure 8*.

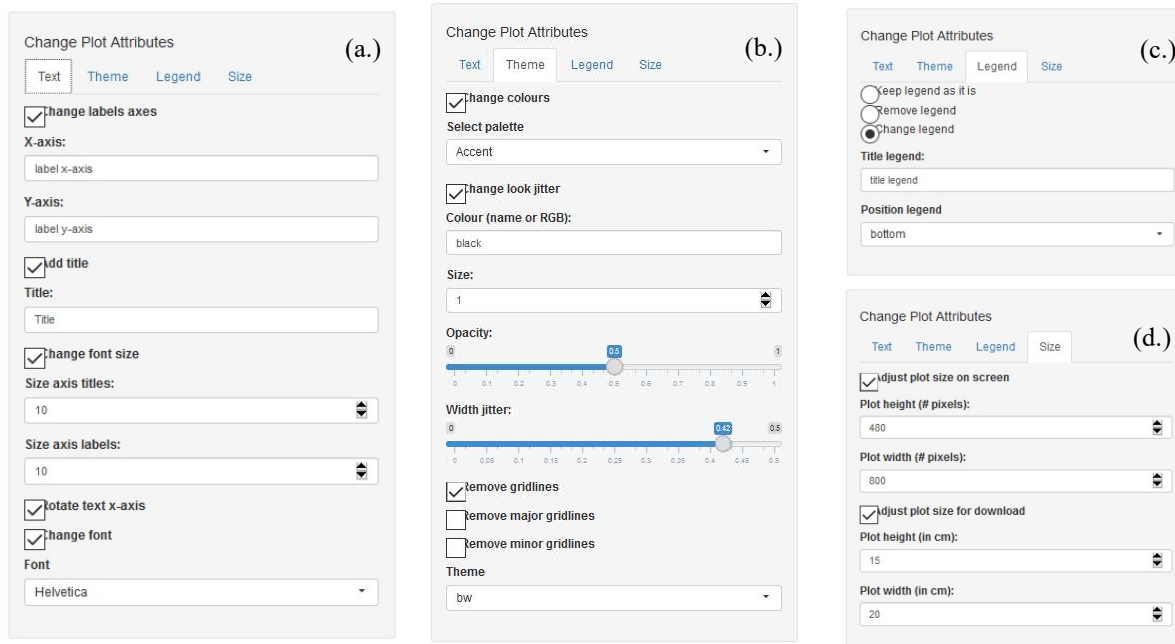


Figure 8. Available plot attribute tools. (a.) Text tab. (b.) Theme tab. (c.) Legend tab. (d.) Size tab

IV. Aluminum-Chlorine-Zirconium Example

In previous studies, Al-Cl-Zr was found to be the most abundant metal-containing aerosol collected by the samplers. Large amounts of this particle class were located in Node 3 of the ISS, which is where crewmembers commonly participate in exercise and personal hygiene. The compound was concluded to be aluminum zirconium tetrachlorohydrate, commonly used in antiperspirant⁴. In this example using the 2016 data, the morphologies of Al-Cl-Zr particles are assessed.

A. Al-Cl-Zr Morphology

First, Al and Cl are plotted as a scatter plot, then further grouped by particle class content. A cluster which contains Al, Cl, and Zr is clearly shown in *Figure 9*.

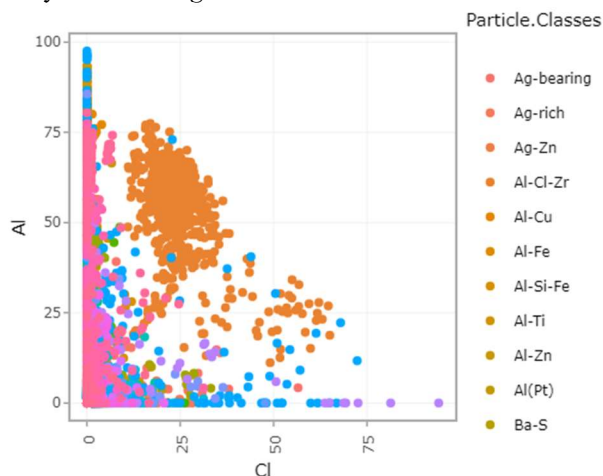


Figure 9. Al-Cl-Zr cluster, shown in orange.

We further seek to assess any potential morphology trends within the Al-Cl-Zr cluster. This is achieved by creating box-and-whisker plots for each of the morphological parameters. According to ASTM “Standard Practice for Characterization of Particles”⁹ and the IntelliSEM user manual⁸, the parameters are defined as follows:

Aspect Ratio:
$$AR = d_{max}/d_{min} \quad (1)$$

Where d_{max} is the longest straight line that can be drawn between any two points on the outline of the particle and d_{min} is the longest line perpendicular to d_{max}

Roundness:
$$R = (4A)/(\pi d_{max}^2) \quad (2)$$

Where A is area and d_{max} is the maximum diameter.

Average Diameter: D_{avg} is determined using the Feret Box method, which involves rotating a box around the particle and recording each measurement. IntelliSEM uses a total of 90 measurements.

Volume:
$$V = \frac{4}{3} \pi \left(\frac{D_{avg}}{2}\right)^3 \quad (3)$$

Volume is estimated using the equation for volume of a sphere and the average diameter of the particle.

Box-and-whisker plots of the different morphological parameters are shown in *Figure 10*.

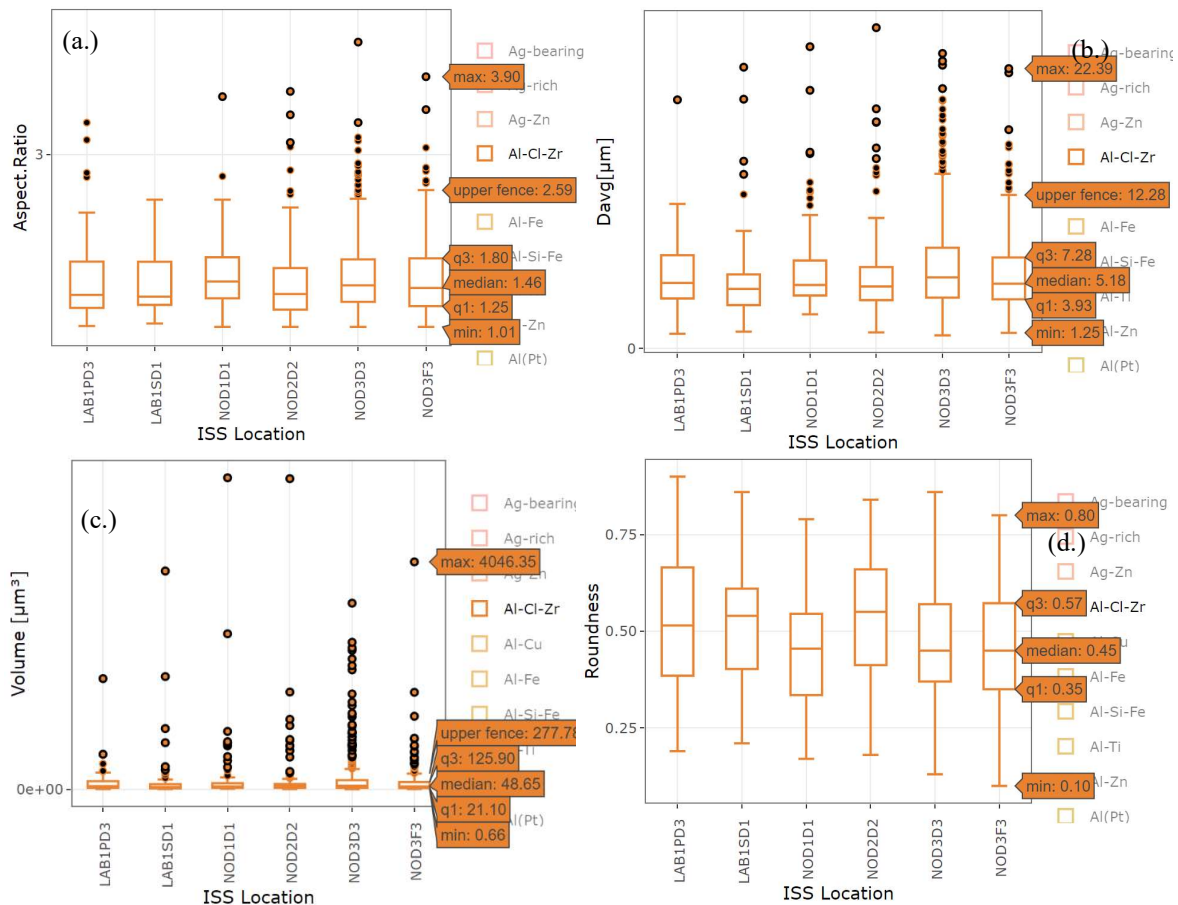


Figure 10. Box-and-whisker plots of Al-Cl-Zr morphology based on ISS location. (a.) Aspect ratio (b.) Average diameter (c.) Volume (d.) Roundness.

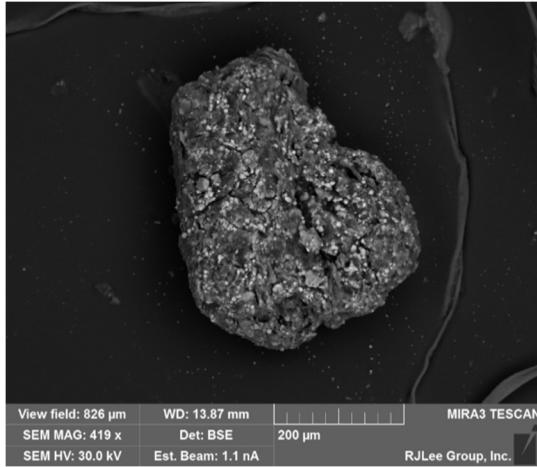


Figure 11. SEM image of a large carbon-based particle with many embedded Al-Cl-Zr particles (the bright inclusions).

PM10 refers to particulate matter under 10 microns. These particles can have health effects on humans as they are able to be inhaled and can penetrate into the respiratory system¹⁰. Given that the average particle diameter for Al-Cl-Zr particles is approximately 5 micrometers, this makes them a likely candidate for inhalation by crewmembers, if they are free-floating individual particles. The small size of the particles may also be damaging to equipment¹¹ aboard the ISS, especially if they are irregularly shaped. Given the median aspect ratio is approximately 1.4 and the median roundness is approximately 0.5, we can conclude most of the Al-Cl-Zr particles are likely globular shaped, as demonstrated in *Figure 11*. Note that the bright inclusions within in the particle depicted here are the Al-Cl-Zr particles, so 5 micrometer particles would not be free-floating in this case. When particles agglomerate into larger particles or are part of a larger structure (greater than *PM10*), they can easily be stopped by the nose and will not enter the body, however they are considered nuisance particles.

V. Lead Content Example

As a more novel example to show the utility of the web application in locating specific particles, lead (Pb) presence on the ISS is shown. Despite only making up a small fraction of the total particles samples, Pb can have significant health effects¹². In this analysis, we locate particles with the largest lead content to estimate abundance, and particles under 10 microns to assess the risk of inhaling such particles.

A. Lead on the ISS

Figure 11 shows Pb % plotted on the y-axis, ISS location plotted on the x-axis, and grouping of particle classes by color for the 2016 data set. Upon inspection, it is seen that several particles have Pb percentages greater than 20%, with one particle in particular containing up to 81.62% Pb. To estimate the abundance of lead, Pb and particle volume are plotted in *Figure 12*.

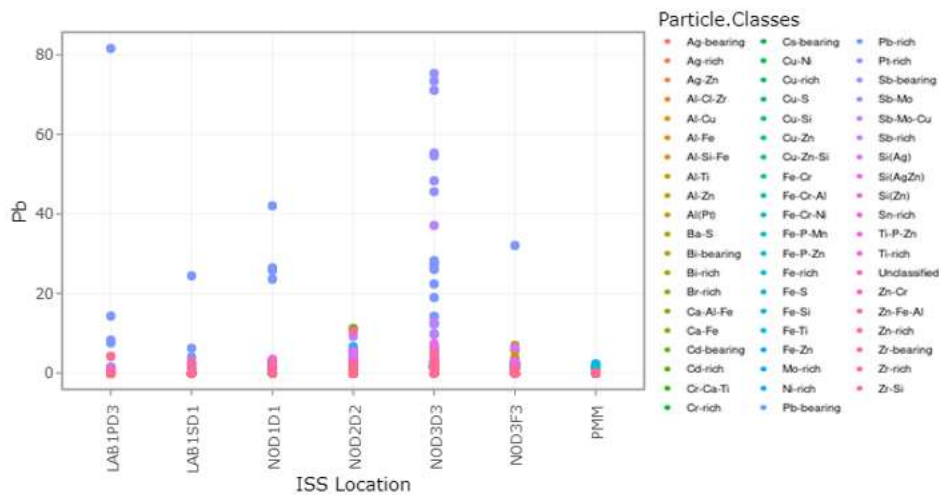


Figure 12. 2016 data for Pb percentage per particle plotted with ISS location and grouped by particle class.

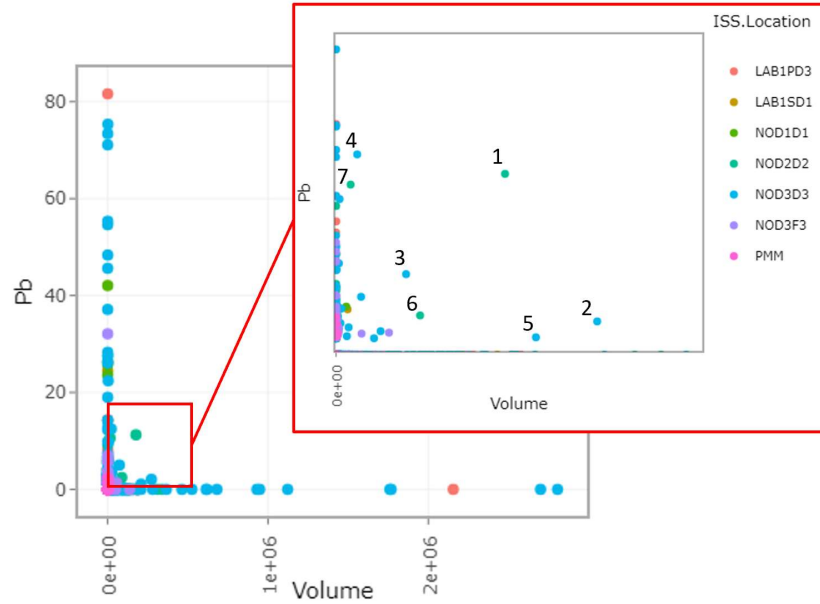


Figure 13. Zoomed in Plot of Pb and volume, grouped by ISS location (2016 data). Numbers show particles ordered by largest amount of Pb, by mass.

To calculate the mass of each particle, *Equation 4* is used. The results of the calculation are shown in *Table 2*.

$$m_{particle} = Percent_{Pb} \times V_{particle} \times Density_{Pb} \quad (4)$$

Table 2. Pb percent, particle volume, and mass of Pb per particle from *Figure 12*.

PARTICLE NUMBER	SAMPLING LOCATION	PB PERCENT (%)	VOLUME OF PARTICLE(μM^3)	MASS OF PB (G)
1	NOD2D2	11.25	176453	22.53
2	NOD3D3	2.07	272713	6.41
3	NOD3D3	5.01	73115	4.16
4	NOD3D3	12.46	22039	3.12
5	NOD3D3	1.08	208746	2.56
6	NOD2D2	2.44	87739	2.43
7	NOD2D2	10.58	15189	1.82

The majority of significant lead-containing particles are located on Node 2 and Node 3, as demonstrated in *Figure 12*.

Another concern regarding lead is its ability to be inhaled by crewmembers. To estimate the mass of inhalable particles, Pb and average diameter are plotted in *Figure 13*. Furthermore, we focus on those particles with diameters under 10 microns and a Pb percentage greater than 40%.

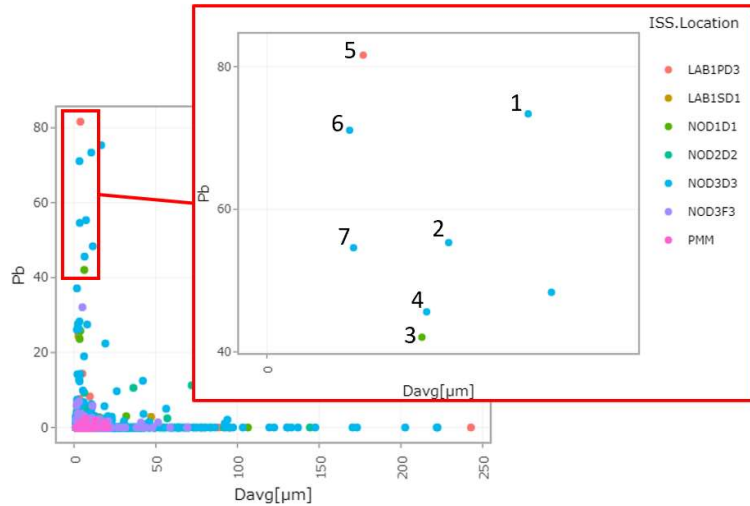


Figure 14. Zoomed in plot of Pb and average diameter. Numbers show particles ordered by largest amount of Pb, by mass.

Once again, the mass of lead in each particle is calculated using *Equation 4*. The results of these calculations as well as exact data for each particle is presented in *Table 3*.

Table 3. Pb percent, particle volume, average particle diameter, and mass of Pb per particle from *Figure 13*.

PARTICLE NUMBER	SAMPLING LOCATION	PB PERCENT (%)	AVERAGE PARTICLE DIAMETER (μM)	PARTICLE VOLUME (μM^3)	MASS PB(MG)
1	NOD3D3	73.39	10.55	329.68	2.73E-03
2	NOD3D3	55.33	7.34	126.01	7.87E-04
3	NOD1D1	42.06	6.26	101.6	4.82E-04
4	NOD3D3	45.62	6.45	89.38	4.60E-04
5	LAB1PD3	81.62	3.89	28.47	2.62E-04
6	NOD3D3	71.09	3.34	12.31	9.88E-05
7	NOD3D3	54.61	3.5	10.59	6.53E-05

B. Possible Lead Sources and Implications

Since the 1990s, many United States military specifications require using approximately 2-3% Pb in tin coatings and solders¹³ as a result of the electronic failures associated with the formation of tin whiskers. Additionally, the Restriction of Hazardous Substances Directive (RoHS), which prohibits the use of lead in electronics in the EU, was not implemented until July 1st 2006. Despite the reduction in lead from supplier electronics, the U.S. has yet to implement regulations preventing the use of lead in electronics¹⁴. It is therefore plausible that electronics containing lead are still in use on the ISS. Some representative particles were imaged separately by manual microscopy in high-resolution micrographs with the corresponding EDS spectra. One such micrograph is shown in *Figure 12*, which demonstrates a lead-containing particle located in the US Lab from the 2016 sampling experiment. While mostly comprised of aluminum, this particle contains both a Pb-Sn-Bi (Cu) inclusion and a Pb-rich inclusion. The presence of these metals commonly found in electronic components (Al, Pb, Sn, Cu) indicate the particle is likely from an

electronic source. As in the example of Figure 11, the Pb particle is not free-floating in this case and has agglomerated onto a larger particle. Therefore it would not be considered PM10 and is not inhalable.

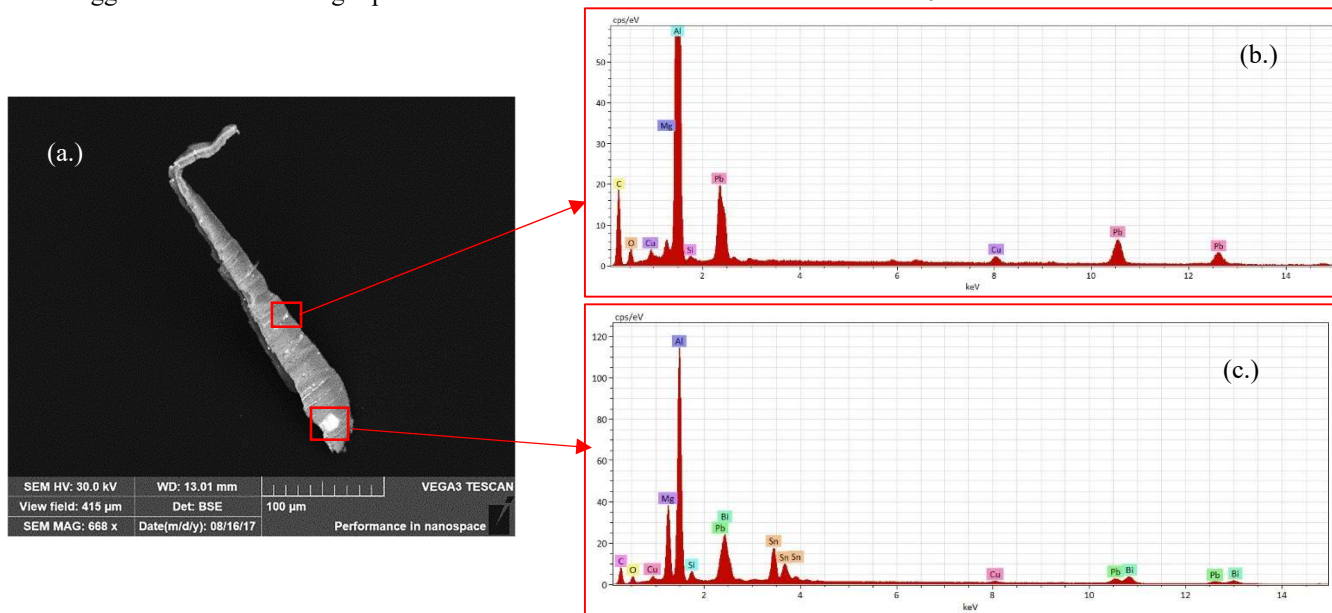


Figure 15. (a.) SEM micrograph from manual microscopy of aluminum silver with Pb and Pb-Sn-Bi(Cu) inclusions. (b.) EDS spectrum of defined region within the particle showing Pb-rich inclusion. (c.) EDS spectrum of defined region within the particle showing Pb-Sn-Bi(Cu) inclusion.

The OSHA permissible exposure limits on lead are defined as $50 \mu\text{g}/\text{m}^3$ over an 8 hour period¹⁵. While a concurrent study calculated an estimate of the airborne concentration of lead in the ISS to be approximately 0.001% of the OSHA limit¹⁶, the number of sub 10 micron particles containing significant percentages of lead should be noted in future aerosol sampling data to gauge whether the emissions are sporadic or relatively consistent, and are not increasing.

VI. Conclusion

The CCSEM and EDS analyses of the samplers from the 2016 and 2018 aerosol sampling experiments produced an abundance of particle composition and morphology data. As a result of this dataset, the ISS Particle Database website was created. The features of the application include elemental composition pie charts (by weight percent) and powerful plotting and interactive plotting tools. These tools allow for the plotting of the nearly 54,500 metal particles (and metal inclusions in larger particles) analyzed and their characteristics, including size, elemental composition and morphology. Additionally, data can be organized by sampling locations, durations, and particle classes. This data was the foundation for future aerosol experiments on ISS, such as the Airborne Particulate Monitor payload which provided the first real-time particle measurements for the purpose of air quality quantification^{17,18,19}.

The web application's utility is demonstrated with the example case showing the morphology of aluminum zirconium tetrachlorohydrate particles, as well as the presence of lead-containing particles. It is concluded that the likely source of Pb particles on the ISS is from electronic components, such as circuit cards, on the ISS. While the RoHS Directive helped to make Pb-free electronics more of a standard, the U.S. still lacks any legal implication for the use of Pb in electronics. Therefore, it is plausible that lead on the ISS comes from older electronic equipment.

Future work includes the improvement of the database capabilities, therefore there may be differences in format, plotting options and content vs. what is shown in this paper. Further updates can be found on the Aerosol Sampling Experiment webpage²⁰. Ideally, ISS sampling experiments would be repeated periodically for comparison purposes and to expand the data set for better statistics. Additionally, it is anticipated that the public web platform will allow researchers within NASA and outside NASA to study air quality in spacecraft, similar to other public NASA databases.

University professors and high school teachers can create course content and projects in STEM with this tool, and the curious lay person can explore this data to learn about the environment in which astronauts live.

Acknowledgments

This project was funded by the Advanced Exploration Systems Life Support Systems Project. RJ Lee Group samplers and microscopy services were supplied under NASA contract #80NSSC18P2726 and others. USRA work was supported by the NASA Academic Mission Services (NAMS) contract # NNA16BD14C. The website is hosted by the NASA Ames Code-I Managed Cloud Environment.

References

- ¹Izadi, E., 'Best Ride I've been on, ever': British astronaut returns to Earth after historic mission. *The Washington Post*, Jun 2016.
- ²Schlesinger T.P., Rodriguez B.R., Borrego M.A., "International Space Station Crew Quarters On-Orbit Performance and Sustaining", *American Institute of Aeronautics and Astronautics*, AIAA 2013-3515, July 2013
- ³Meyer, M. E., "Data and Results from Aerosol Sampling Experiment on International Space Station," NASA TM-219577, 2018.
- ³Meyer, M. E., "Aerosol Sampling Experiment on the International Space Station," 47th *International Conference on Environmental Systems*, ICES-2017-74, AIAA, Charleston, South Carolina, July 2017.
- ⁴Meyer, M. E., "Results of the Aerosol Sampling Experiment on the International Space Station", 48th *International Conference on Environmental Systems*, ICES-2018-100, AIAA, Albuquerque, New Mexico, July 2018.
- ⁵Meyer, M. E., "Further Characterization of Aerosols Sampled on the International Space Station," 49th *Conference on Environmental Systems*, Boston, Massachusetts, July 2019.
- ⁶Norris, J.S., "Mission-critical development with open source software: lessons learned", *Institute of Electrical and Electronics Engineers* vol. 21, no. 1, Jan-Feb. 2004, , pp.42-49.
- ⁷International Space Station Aerosol Sampling Experiment Database of Particles and Particle Components by Meyer, M.E., Sorek-Hamer, M., Hallinan, I.P.; NASA Advanced Exploration Systems Life Support Systems Project. <https://iss-particle-db.arc.nasa.gov>.
- ⁸RJLee Group, IntelliSEM Workbench Users Manual, March 2019.
- ⁹ASTM Standard F1877 – 16, "Standard Practice for Characterization of Particles," *ASTM International*, West Conshohocken, PA, October 2016.
- ¹⁰Cooper D.C., Alley F.C., Causes, Sources, and Effects Chapter in *Air Pollution Control: A Design Approach* (4th ed., pp. 55 – 53). Waveland Press Inc. Long Grove, IL. 2011.
- ¹¹Zhao Bin, Chen Jiujiu, Li Xianting, Chen Xi. Source, effect and distribution of indoor particulate matter *Journal of Environment and Health*. 2005 ;22(1):65-68.
- ¹²Kosnett MJ. "Lead". In Brent J (ed.). *Critical Care Toxicology: Diagnosis and Management of the Critically Poisoned Patient*. Gulf Professional Publishing. 2005.
- ¹³J. Brusse, H. Leidecker, L. Panashchenko. *Metal Whiskers: Failure Modes and Mitigation Strategies*. MRQW, Dec. 2007
- ¹⁴Kostic A. *Lead-Free Electronics Reliability – An Update*. GEOINT Development Office, Aerospace Corporation, August 2011
- ¹⁵<https://www.osha.gov/laws-regs/regulations/standardnumber/1910/1910.1025>
- ¹⁶Rodell A.J., Li. W., Calle L.M., Meyer M.E., "Presence of Metal Aerosols on the International Space Station," 51st *International Conference on Environmental Systems*, ICES-2022-288, AIAA, St. Paul MN, July 2022.
- ¹⁷Ley, S.E., Li, W., Rodell, A.J., Calle, L.M, Meyer, M.E., Lersch, T., Bunker, K., Casuccio, G. (2021) Fate of Silver Biocide on the International Space Station Living Environment, 50th International Conference on Environmental Systems, July 12, 2021, Virtual, ICES-2021-352.
- ¹⁸Meyer, M. E. (2020) Airborne Particulate Monitor: A Real-time Reference-Quality Aerosol Instrument Payload for ISS Air Pollution Quantification, 50th International Conference on Environmental Systems, 2020, ICES-2020-65, paper published but not presented (no conference due to COVID-19).
- ¹⁹Meyer, M. E. (2022) Lessons Learned from the Airborne Particulate Monitor ISS Payload, 51st International Conference on Environmental Systems, 2022, ICES-2022-311, St. Paul, Minnesota, July 2022.
- ²⁰"Aerosol Sampling Experiment." *Space Station Research Explorer on NASA.gov*. September 2016. https://www.nasa.gov/mission_pages/station/research/experiments/explorer/Investigation.html?id=2034.